

BEYOND CARLEMAN LINEARIZATION OF NONLINEAR DYNAMICAL SYSTEM: INSIGHTS FROM A CASE STUDY

PANPAN CHEN, NADER MOTEE, AND QIYU SUN

In memory of Jean-Pierre Gabardo

ABSTRACT. Nonlinear dynamical systems are widely encountered in various scientific and engineering fields. Despite significant advances in theoretical understanding, developing complete and integrated frameworks for analyzing and designing these systems remains challenging, which underscores the importance of efficient linearization methods. In this chapter, we introduce a general linearization framework with emphasis on Carleman linearization and Carleman-Fourier linearization. A detailed case study on finite-section approximation to the lifted infinite-dimensional dynamical system is provided for the dynamical system with its governing function being a trigonometric polynomial of degree one.

1. INTRODUCTION

Nonlinear dynamical systems are ubiquitous in disciplines ranging from physics and biology to engineering. Although substantial theoretical progress has been made, holistic mathematical frameworks for the systematic analysis and design of these systems continue to exhibit significant challenges. These methodological gaps highlight the vital importance of enhancing the value of transforming nonlinear systems into linearization frameworks. Over time, it developed into a leading method for analyzing nonlinear systems, driven by advancements in theory, enhanced computational techniques, and data explosion [2, 6, 7, 8, 9, 10, 11, 12, 13, 14, 16, 17, 18, 20, 23, 24, 27, 28, 29, 30, 31]. In this chapter, we consider lifting nonlinear dynamical systems that are described by

$$(1.1) \quad \frac{dx}{dt} = g(x) \quad \text{with} \quad x(0) = x_0,$$

where $t \geq 0$ is the time variable, $x := x(t) \in \mathbb{C}$ represents the state variable, g serves as the governing function, and $x_0 \in \mathbb{C}$ acts as the initial.

We say that a map Ψ is a **lifting operator** of the nonlinear dynamical system (1.1) if the lifted system can be described as a linear dynamical system,

$$(1.2) \quad \frac{d\Psi(x)}{dt} = F(\Psi(x)),$$

This work was partially supported by ONR N00014-23-1-2779.

where $F(y)$ is an affine function about y . For engineering applications, the lifting operator Ψ should be appropriately designed so that the original state variable x can be recovered from its lifting $\Psi(x)$ by some **projection** Φ ,

$$(1.3) \quad x = \Phi(\Psi(x)).$$

Carleman linearization, Carleman-Fourier linearization and Koopman linearization are well-known lifting schemes, where the resulting lifted systems are represented by linear operators on some infinite-dimensional linear space. In this chapter, we consider Carleman linearization and Carleman-Fourier linearization of the dynamical system (1.1) with the governing function g being a trigonometric polynomial, i.e.,

$$(1.4) \quad g(x) = \sum_{m=-M}^M g_m e^{imx}$$

for some constant Fourier coefficients $g_m, -M \leq m \leq M$.

Carleman linearization has lifting and projection operators defined by

$$(1.5) \quad \Psi(x) = [x, x^2, \dots, x^N, \dots]^T \quad \text{and} \quad \Phi[y_1, y_2, \dots, y_N, \dots]^T = y_1.$$

It has been embraced by the control system community in a variety of successful applications, such as optimal nonlinear control design, model predictive control, state estimation and feedback control. These successes underscore the value of Carleman linearization in transforming nonlinear control problems into a linear paradigm, where powerful analytical tools can be applied. This transformation not only facilitates deeper insights into system behavior, but also enables the development of effective control strategies for nonlinear dynamics [4, 5, 8, 12, 15, 19, 20, 21, 22, 24, 25, 26]. The key idea in Carleman linearization is to **decouple** auxiliary variables $x^n, n \geq 1$, which represent higher-order powers of the state variable x . The main challenge is that the state matrix of the lifted infinite-dimensional linear system is the product of a diagonal matrix with **unbounded** diagonal entries and a Laurent matrix with exponential off-diagonal decay, and hence the corresponding infinite-dimensional system is **not amenable** to any of the existing tools for analysis. Carleman linearization is applicable for dynamical systems with the governing function being analytic around the origin, and it can be viewed as the dynamical system counterpart to the Maclaurin expansion for analytic functions. Similar to the behavior of the Maclaurin expansion of an analytic function near the origin, a finite-section approximation to the Carleman linearization with higher orders offers significantly improved accuracy and a broader time range of validity compared to the conventional linearized dynamical model, especially when the dynamical system has the origin as its equilibrium and the initial is not far away from the origin. In Section 2, we consider Carleman linearization of the dynamical system (1.1) with the trigonometric polynomial governing function g in (1.4), and we present numerical demonstration for the Carleman linearization of

the illustrative dynamical system with governing function

$$(1.6) \quad g(x) = a(1 - e^{ix})$$

for some nonzero $0 \neq a \in \mathbb{C}$. As the dilated state $x(t/|a|)$ and the reflected state $-\Re x + i\Im x$ satisfy (1.6) with the parameter a replaced by $a/|a|$ and $-\Re a + i\Im a$, respectively, we may normalize the dynamical system (1.6) so that

$$(1.7) \quad a = e^{i\phi} \text{ for some } \phi \in [-\pi/2, \pi/2].$$

Here and hereafter, we denote the real and imaginary parts of a complex number $z \in \mathbb{C}$ by $\Re z$ and $\Im z$ respectively. With the normalization (1.7) on the parameter a , one may verify that the dynamical system (1.1) with the governing function (1.6) has the origin as an equilibrium and its solution can be explicitly expressed as

$$(1.8) \quad x(t) = at + x_0 + i \ln(1 + (e^{ait} - 1)e^{ix_0})$$

in a short time period, see Appendix A. Here we use $\text{Arg}(z) \in (-\pi, \pi]$ to denote the angle of a nonzero complex number $z \neq 0$, and set $\ln(z) = \ln|z| + i\text{Arg}(z)$.

As the governing function g in (1.4) exhibits periodic behavior, a natural linearization of the dynamical system (1.1) is to adopt the Fourier system $\{e^{ix}, e^{-ix}, e^{2ix}, e^{-2ix}, \dots\}$, instead of $\{x, x^2, \dots\}$ in the Carleman linearization (2.3). However, the state matrix of the associated linearization (3.1) does not have an upper triangular structure, which is crucial for the convergence analysis in the Carleman linearization; see Theorem 2.1. This highlights the critical need to reassess the linearization approach for the nonlinear dynamical system (1.1). In Section 3, we introduce Carleman-Fourier linearization to the nonlinear dynamical system (1.1) with governing function g in (1.4). The Carleman-Fourier linearization in (3.8) is based on the observation that the dynamical system associated with the extended state vector $\mathbf{x} = [x_1, x_2]^T$, **decoupled** from state variables $x_1 = x$ and $x_2 = -x$, has its governing field being a trigonometric polynomial with nonnegative frequencies only. The proposed Carleman-Fourier linearization (3.8) has lifting and projection operators defined by

$$(1.9) \quad \Psi(x) = [\exp(i\boldsymbol{\alpha}^T \mathbf{x})]_{\boldsymbol{\alpha} \in \mathbb{Z}_{++}^2} \text{ and } \Phi([y_{\boldsymbol{\alpha}}]_{\boldsymbol{\alpha} \in \mathbb{Z}_{++}^2}) = -i \ln y_{[1,0]},$$

where $\mathbf{x} = [x, -x]^T$ and \mathbb{Z}_{++}^2 is the set of all nonzero pairs of nonnegative integers. The linearization proposed in (3.8) inherently preserves the structure of the triangular matrix of the upper block, allowing mathematically tractable and rigorous convergence analysis. Furthermore, it is well-adapted to dynamical systems governed by periodic vector functions, leading to a more structured and efficient embedding of periodic nonlinear dynamics within a linear framework; see Section 4.

For the case that the governing function g in (1.4) has a nonnegative frequency only, i.e., (3.9) holds, the Carleman-Fourier linearization in (3.8) can be reduced to a scaled form for each block. In particular, we may employ the following lifting and

projection operators:

$$(1.10) \quad \Psi(x) = [\exp(ix), \exp(2ix), \dots]^T \quad \text{and} \quad \Phi([z_1, z_2, \dots]^T) = -i \ln z_1.$$

Since both the lifted vector and state matrix in the concise formulation (3.11) are subsets of their counterparts in the Carleman-Fourier linearization described in (3.8), we maintain using the terminology of Carleman-Fourier linearization for the resulting system (3.11). For our case study with the governing function in (1.6), we observe that the state matrix in the corresponding Carleman-Fourier linearization exhibits an upper-triangular structure with bandwidth one, see (3.13).

The state matrix \mathbf{B} in the proposed Carleman-Fourier linearization (3.8) does not constitute a bounded operator in $\ell^2(\mathbb{Z}_{++}^2)$ which consists of all square-summable sequences on \mathbb{Z}_{++}^2 . This lack of boundedness prevents the direct application of the standard theories for Hilbert space dynamical systems to analyze the lifted system and, by extension, the original nonlinear dynamical system. An alternation to explore the infinite-dimensional lifted system (3.8) is its finite-section approximation, see (4.1). In Theorem 4.1, we show that the first block in the finite-section approximation (4.1) converges to the exponential of the extended state vector over some time range. For the governing function in (1.6), we derive an explicit solution of the dynamical system associated with the corresponding finite-section approximation; see (5.1). As a sequence, the first component in the finite-section approximation is essentially the Maclaurin polynomial of the exponential of the original state in (1.8), and hence we have the explicit formula for its exponential convergence rate and time range; see (5.3) and (5.7).

This chapter is organized as follows. In Section 2, we present the Carleman linearization framework for the nonlinear dynamical system (1.1) with the governing function g given in (1.4), see (2.3). Also we numerically demonstrate the exponential convergence of finite-section approximations to the Carleman linearization when the governing function g is specified in (1.6), see Theorem 2.1 and Figures 1 and 2. In Section 3, we introduce the Carleman-Fourier linearization with extended variables method, see (3.8). This approach removes exponential terms with negative frequencies from the original nonlinear system, and transforms it into an infinite-dimensional linear system whose state matrix has a block-upper triangular structure. A concise version of Carleman-Fourier linearization is also discussed when the governing function has nonnegative frequencies only, see (3.11). In Section 4, we consider the finite-section approximation of the Carleman-Fourier system (3.8), providing a computationally tractable finite-dimensional alternative and an effective method for approximating nonlinear dynamical systems. We show that the first block in the finite-section approximation has exponential convergence to the exponential of the state variable in the original dynamical system over a specified time range. To illustrate the Carleman-Fourier linearization, in Section 5 we derive an exact time range and convergence rate for the finite-section approximation with the governing function in

(1.6). Our numerical demonstrations indicate that the Carleman-Fourier linearization outperforms standard Carleman linearization when the imaginary part of the initial state takes a large value, while Carleman linearization remains superior for systems with initial states near the origin.

2. CARLEMAN LINEARIZATION

In this section, we consider Carleman linearization of the nonlinear dynamical system described in (1.1) with the governing function g given in (1.4), and discuss the exponential convergence of the first component in the finite-section approximation to the state variable of the original dynamical system (1.1), see (2.3) and Theorem 2.1. The reader may refer to [1, 2, 3, 11, 18, 20, 27, 31] and references therein for the Carleman linearization of nonlinear dynamical systems with the governing vector fields being analytic around the origin.

The key idea in Carleman linearization is to decouple auxiliary variables $x^n, n \geq 1$, that represent higher-order powers of the state variable x . With Maclaurin expansion

$$(2.1) \quad g(x) = \sum_{m=-M}^M g_m \sum_{n=0}^{\infty} \frac{(imx)^n}{n!} =: \sum_{n=0}^{\infty} c_n x^n$$

for the governing trigonometric polynomial g in (1.4), we obtain from (1.1) that

$$(2.2) \quad \frac{dx^n}{dt} = nx^{n-1} \frac{dx}{dt} = nx^{n-1} g(x) = n \sum_{n'=n-1}^{\infty} c_{n'-n+1} x^{n'}, \quad n \geq 1.$$

Grouping the above ODEs together yields the following infinite-dimensional linear system of ODEs,

$$(2.3) \quad \frac{d\mathbf{x}}{dt} = \mathbf{Ax} + \mathbf{a},$$

where $\mathbf{x} = [x, x^2, \dots, x^N, \dots]^T$, $\mathbf{a} = [c_0, 0, \dots, 0, \dots]^T$, and the state matrix $\mathbf{A} = [nc_{n'-n+1}]_{n,n'=1}^{\infty}$ is given by

$$(2.4) \quad \mathbf{A} = \begin{bmatrix} c_1 & c_2 & \cdots & c_{N-1} & c_N & \cdots \\ 2c_0 & 2c_1 & \cdots & 2c_{N-2} & 2c_{N-1} & \cdots \\ 3c_0 & \cdots & 3c_{N-3} & 3c_{N-2} & \cdots & \cdots \\ \ddots & \vdots & \vdots & \ddots & \ddots & \ddots \\ Nc_0 & Nc_1 & \ddots & & & \ddots \end{bmatrix}.$$

We call the infinite-dimensional dynamical system (2.3) obtained from decoupling $x^n, n \geq 1$, as **Carleman linearization** of the nonlinear dynamical system (1.1).

The state matrix \mathbf{A} in the Carleman linearization (2.3) is the product of a diagonal matrix with unbounded entries and a Laurent matrix with exponential off-diagonal decay,

$$\mathbf{A} = \begin{bmatrix} 1 & & & & & & \\ & 2 & & & & & \\ & & 3 & & & & \\ & & & \ddots & & & \\ & & & & N & & \\ & & & & & \ddots & \\ & & & & & & \ddots \end{bmatrix} \begin{bmatrix} c_1 & c_2 & \cdots & c_{N-1} & c_N & \cdots \\ c_0 & c_1 & \cdots & c_{N-2} & c_{N-1} & \cdots \\ c_0 & \cdots & c_{N-3} & c_{N-2} & \cdots \\ \ddots & & \vdots & \vdots & \ddots \\ c_0 & c_1 & & & \ddots \\ & & \ddots & & \ddots \end{bmatrix}.$$

It is an upper-triangular matrix when the origin is an equilibrium of the nonlinear dynamical system (1.1), i.e.,

$$(2.5) \quad g(0) = c_0 = 0.$$

By exploiting the upper triangular structure of the state matrix \mathbf{A} and building on techniques developed in [2], we may use the following **finite-section approximation** framework to approximate the infinite-dimensional linear dynamical system (2.3),

$$(2.6) \quad \frac{d\mathbf{x}_N}{dt} = \mathbf{A}_N \mathbf{x}_N + \mathbf{a}_N$$

with the initial condition $\mathbf{x}_N(0) = [x_0, x_0^2, \dots, x_0^N]^\top$, where $\mathbf{x}_N = [x_{1,N}, \dots, x_{N,N}]^\top$, $\mathbf{a}_N = [c_0, \dots, 0]^T$, and the state matrix

$$\mathbf{A}_N = \begin{bmatrix} c_1 & c_2 & \cdots & c_{N-1} & c_N \\ 2c_0 & 2c_1 & \cdots & 2c_{N-2} & 2c_{N-1} \\ 3c_0 & \cdots & 3c_{N-3} & 3c_{N-2} \\ \ddots & \vdots & & \vdots \\ Nc_0 & & Nc_1 \end{bmatrix} = \begin{bmatrix} 1 & & & & & \\ & 2 & & & & \\ & & \ddots & & & \\ & & & N & & \\ & & & & & \end{bmatrix} \begin{bmatrix} c_1 & c_2 & \cdots & c_{N-1} & c_N \\ c_0 & c_1 & \cdots & c_{N-2} & c_{N-1} \\ c_0 & \cdots & c_{N-3} & c_{N-2} \\ \ddots & & \vdots & \vdots \\ c_0 & c_1 \end{bmatrix}$$

is the leading $N \times N$ principal submatrix of the state matrix \mathbf{A} of the Carleman linearization. Unlike the infinite-dimensional system setting, we observe that $x_{k,N}, 1 \leq k \leq N$ in the finite-dimensional system above does not **not** satisfy the coupling property $x_{k,N} = (x_{1,N})^k, 1 \leq k \leq N$. We also notice that the finite-dimensional dynamical system (2.6) with $N = 1$ is the conventional linearized dynamical model at the origin,

$$(2.7) \quad \frac{dx_1}{dt} = c_0 + c_1 x_1 = g(0) + g'(0)x_1.$$

In this regard, we may view the Carleman linearization and its finite-section approximation as an **analogue** of the Maclaurin expansion for an analytic function and its Maclaurin polynomial approximation in the context of dynamical systems.

Stated in the following theorem is that the first component $x_{1,N}(t)$ for $N \geq 1$, in the finite-section approximation (2.6) provides an exponential approximation to the solution $x(t)$ of the original dynamical system (1.1) in a short time range, provided that the origin is an equilibrium of the dynamical system, i.e., (2.5) holds.

Theorem 2.1. *Consider the dynamical systems*

$$(2.8) \quad \frac{dx}{dt} = f(x)$$

with the governing function f being an analytic function with Maclaurin expansion

$$f(x) = \sum_{n=1}^{\infty} c_n x^n$$

and Maclaurin coefficients satisfying

$$(2.9) \quad |c_n| \leq C_0 \frac{R_0^{n-1}}{n!}, \quad n \geq 1,$$

for some positive constants C_0 and R_0 , and let $x_{1,N}$ be the first component of the state vector in the finite-section approximation of order N to its Carleman linearization (2.3). Then

$$(2.10) \quad |x_{1,N}(t) - x(t)| \leq \frac{\tilde{R}_0 e^{\tilde{R}_0}}{\sqrt{2\pi} R_0} N^{-3/2} \left(\frac{R_0 |x_0| e^{C_0(1+1/\tilde{R}_0)e^{\tilde{R}_0}t}}{\tilde{R}_0} \right)^N$$

holds for all $0 \leq t \leq T^$ and $N \geq 1$, where*

$$(2.11) \quad \tilde{R}_0 = \max(1, R_0 |x_0| e^2)$$

and

$$(2.12) \quad T^* = \frac{\tilde{R}_0}{C_0(\tilde{R}_0 + 1)e^{\tilde{R}_0}} \min \left(\ln \frac{\tilde{R}_0}{e R_0 |x_0|}, 2 \right).$$

We follow the argument in [2] to prove Theorem 2.1. For the completeness of this chapter, we include a sketch proof in Appendix B.

For the governing function g in (1.6), the corresponding Carleman linearization (2.3) is homogeneous (i.e., $\mathbf{a} = \mathbf{0}$) and has the upper triangular state matrix

$$(2.13) \quad \mathbf{A} = -a \begin{bmatrix} i & \frac{i^2}{2!} & \cdots & \frac{i^{N-1}}{(N-1)!} & \frac{i^N}{N!} & \cdots \\ 2i & \cdots & \frac{2i^{N-2}}{(N-2)!} & \frac{2i^{N-1}}{(N-1)!} & \cdots & \\ \ddots & & \vdots & \vdots & \ddots & \\ & & (N-1)i & \frac{(N-1)i^2}{2!} & \cdots & \\ & & & \frac{Ni}{N!} & \cdots & \\ & & & & \ddots & \end{bmatrix},$$

and its finite-section approximation is given by

$$(2.14) \quad \frac{d}{dt} \begin{bmatrix} x_{1,N}(t) \\ x_{2,N}(t) \\ \vdots \\ \vdots \\ x_{N-1,N}(t) \\ x_{N,N}(t) \end{bmatrix} = -a \begin{bmatrix} i & \frac{i^2}{2!} & \cdots & \cdots & \frac{i^{N-1}}{(N-1)!} & \frac{i^N}{N!} \\ 2i & \cdots & \cdots & \cdots & \frac{2i^{N-2}}{(N-2)!} & \frac{2i^{N-1}}{(N-1)!} \\ \ddots & \ddots & \ddots & \ddots & \vdots & \vdots \\ \ddots & \ddots & \ddots & \ddots & \vdots & \vdots \\ (N-1)i & \cdots & \cdots & \cdots & \frac{(N-1)i^2}{2!} & \cdots \\ & & & & \frac{Ni}{N!} & \cdots \end{bmatrix} \begin{bmatrix} x_{1,N}(t) \\ x_{2,N}(t) \\ \vdots \\ \vdots \\ x_{N-1,N}(t) \\ x_{N,N}(t) \end{bmatrix}$$

with initial $x_{k,N}(0) = x_0^k$ for $1 \leq k \leq N$. Due to the upper triangular property of the state matrix, the above linear system can be solved by a set of scale-valued ODEs:

$$\frac{dx_{N,N}}{dt} = -Naix_{N,N} \quad \text{with} \quad x_{N,N} = x_0^N$$

and

$$\frac{dx_{k,N}}{dt} = -kaix_{k,N} - ka \sum_{k'=k+1}^N \frac{i^{k'-k+1}}{(k'-k+1)!} x_{k',N} \quad \text{with} \quad x_{k,N}(0) = x_0^k$$

inductively for $k = N-1, \dots, 1$.

For the dynamical system with the governing function g given in (1.6), the requirement (2.9) in Theorem 2.1 is satisfied with $C_0 = |a| = 1$ and $R_0 = 1$. Hence as a consequence of Theorem 2.1,

$$(2.15) \quad |x_{1,N}(t) - x(t)| \leq (2\pi)^{-1/2} \tilde{R}_0 e^{\tilde{R}_0} N^{-3/2} \left(\frac{|x_0|e}{\tilde{R}_0} e^{e^{\tilde{R}_0}(1+1/\tilde{R}_0)t} \right)^N$$

hold for all $0 \leq t \leq \frac{\tilde{R}_0}{(\tilde{R}_0+1)e^{\tilde{R}_0}} \min \left(\ln \frac{\tilde{R}_0}{|x_0|e}, 2 \right)$, where $x_{1,N}$ is the first component of the state vector in (2.14), and $\tilde{R}_0 = \max(1, |x_0|e^2)$. Shown in Figure 1 is the approximation error measurement

$$(2.16) \quad E_C(x_0, T^*, N) = \max_{0 \leq t \leq T^*} \log_{10} |e^{i(x_{1,N}(t) - x(t))} - 1|,$$

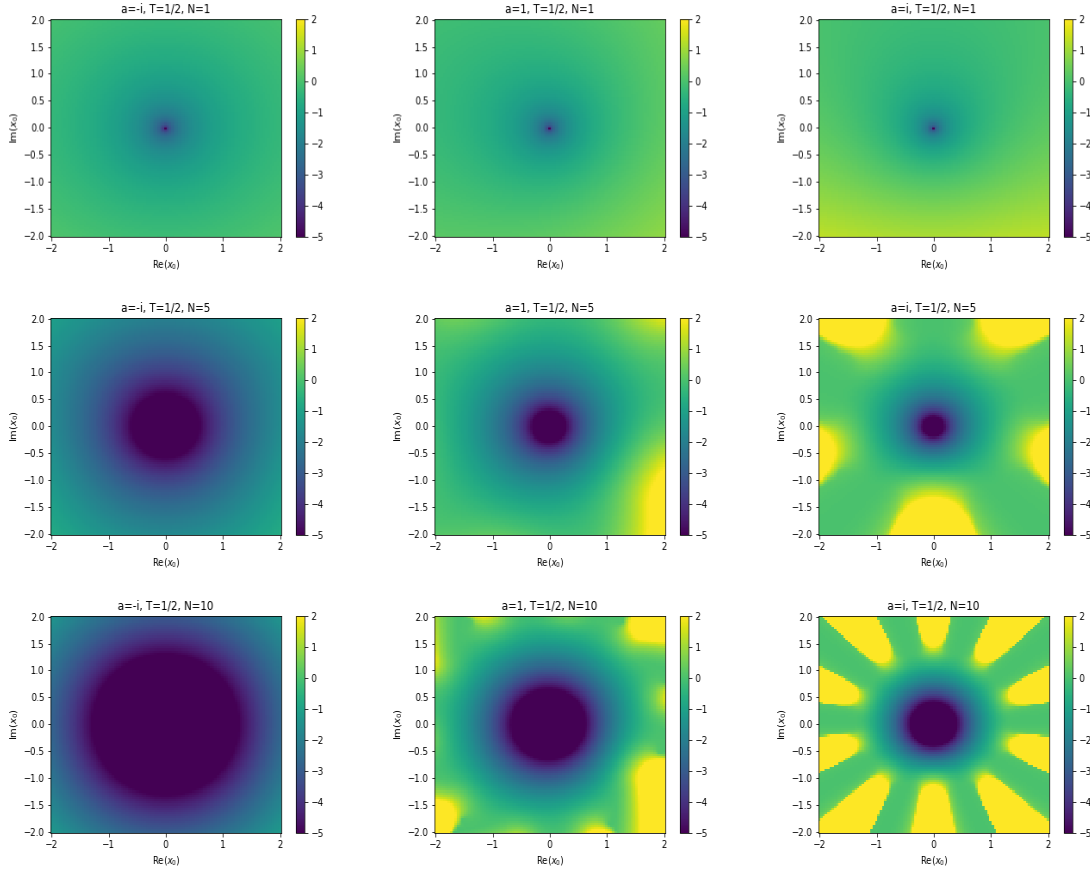


FIGURE 1. The figures above display the finite-section approximation errors, given by $\max(\min(E_C(x_0, T^*, N), 2), -5)$ in (2.16), over the domain $-2 \leq \Re x_0, \Im x_0 \leq 2$, with a fixed time range $T^* = 1/2$. The columns correspond to value $a = -i$ (left), 1 (middle), and i (right), while the rows correspond to $N = 1$ (top), 5 (middle), and 10 (bottom).

where the initial x_0 is selected in the domain $[-2, 2] + [-2, 2]i$, and $a = -i, 1, i$ from left to right, and $N = 1, 5, 10$ from top to bottom. A comparison of figures across rows reveals that, as expected, the finite-section approximation achieves higher accuracy when the initial value is close to the origin (where the governing function is well-approximated by polynomials of low degrees), and the approximation error further decreases as the truncation order N increases, provided that the finite-section approximation converges. On the other hand, the first component of the finite-section approximation fails to approximate the original state vector for initial values far from the origin. Comparing column-wise results, we observe that the finite-section

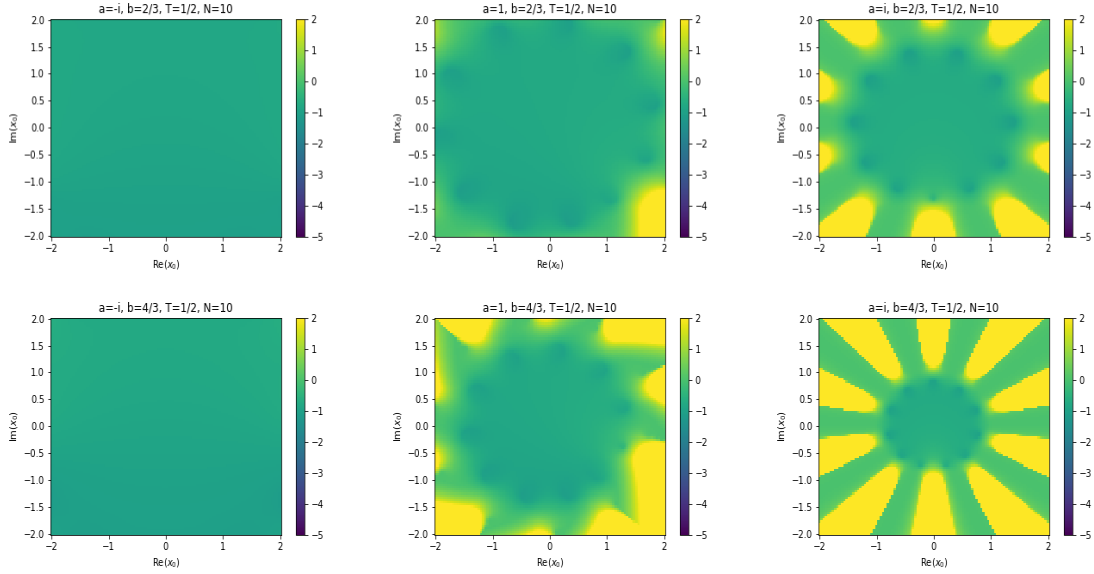


FIGURE 2. The finite-section approximation errors, given by $\max(\min(E_C(x_0, T^*, N), 2), -5)$ in (2.16), over the domain $-2 \leq \Re x_0, \Im x_0 \leq 2$, with a fixed time range $T^* = 1/2$ and truncation order $N = 10$. The columns correspond to value $a = -i$ (left), 1 (middle), and i (right), while the rows correspond to value $b = 2/3$ (top) and $b = 4/3$ (bottom).

approximation performs more effectively for $a = -i$ in which where the origin is a stable equilibrium than for $a = i$ where the origin is an unstable equilibrium.

Consider the dynamical system

$$(2.17) \quad \frac{dx}{dt} = a(1 - be^{ix}), \quad t \geq 0$$

with $0 \neq a, b \in \mathbb{C}$, which reduces to the dynamical system (1.6) when $b = 1$ is selected. The dynamical system (2.17) has the origin as its equilibrium if and only if $b = 1$. Shown in Figure 2 is the approximation error of the finite-section approach to its Carleman linearization with $b = 2/3$ and $4/3$. Compared with the numerical results shown in Figure 1 where the origin is an equilibrium point, the finite-section approximation shown in Figure 2 exhibits slower convergence when the initial condition x_0 lies near the origin; however, it still achieves exponential convergence over a finite time interval, even though the origin is not an equilibrium point. We conjecture that such exponential convergence property could be mathematically proved for the finite-section approximation to the Carleman linearization of the dynamical system (1.1) under the assumption that the parameter $g(0)$ is close to zero (where the state matrix \mathbf{A} in (2.4) is no longer an upper triangular matrix). The main challenge is that

the conventional perturbation approach is not directly applicable due to the presence of an unbounded operator in the infinite-dimensional lifted system

3. CARLEMAN-FOURIER LINEARIZATION

In this section, we consider Carleman-Fourier linearization for the nonlinear dynamical system described in (1.1) with the governing function g given in (1.4). The extended Carleman-Fourier linearization framework for nonlinear dynamical systems with governing fields having multiple fundamental frequencies can be found in [10, 23].

Let \mathbb{Z}_0 be the set of all nonzero integers. The classical Carleman linearization approach, based on monomial functions $x^n, n \geq 1$, can be naturally extended to the dynamical system (1.1) with periodic governing function g in (1.4), by considering the derivatives of the Fourier basis $e^{inx}, n \in \mathbb{Z}_0$. By (1.1) and (1.4), we have

$$\frac{de^{inx}}{dt} = ine^{inx} \frac{dx}{dt} = in \sum_{m=-M}^M g_m e^{i(n+m)x}, \quad n \in \mathbb{Z}_0.$$

Combining the above ODEs together yields the following linearization of the nonlinear dynamical system (1.1),

$$(3.1) \quad \frac{d\mathbf{w}}{dt} = \mathbf{H}\mathbf{w} + \mathbf{h},$$

where $\mathbf{w} = [e^{inx}]_{n \in \mathbb{Z}_0}$ is the state vector, the state matrix $\mathbf{H} = [in g_{n'-n}]_{n, n' \in \mathbb{Z}_0}$ and nonhomogenous term $\mathbf{h} = [in g_{-n}]_{n \in \mathbb{Z}_0}$ are given by

$$(3.2) \quad \mathbf{H} = \begin{bmatrix} \dots & \vdots & \vdots & \vdots & \vdots & \vdots & \dots \\ \dots & 2ig_0 & 2ig_{-1} & 2ig_{-3} & 2ig_{-4} & \dots \\ \dots & 2ig_0 & 2ig_{-1} & 2ig_{-3} & 2ig_{-4} & \dots \\ \dots & ig_1 & ig_0 & ig_{-2} & ig_{-3} & \dots \\ \dots & -ig_3 & -ig_2 & -ig_0 & -ig_{-1} & \dots \\ \dots & -2ig_4 & -2ig_3 & -2ig_1 & -2ig_0 & \dots \\ \vdots & \vdots & \vdots & \vdots & \vdots & \vdots & \vdots \end{bmatrix},$$

and

$$\mathbf{h} = [\dots, 2ig_{-2}, ig_{-1}, -ig_1, -2ig_2, \dots]^T$$

respectively. The above linearization captures the periodicity of the governing function g in (1.4). However, unlike in the Carleman linearization, the state matrix \mathbf{H} in the current linearization approach does not maintain an upper triangular form, which is crucial to our convergence analysis in Theorem 2.1. This fundamental difference highlights the need to reconsider the linearization strategy for the dynamical system (1.1) with the governing function g given in (1.4).

Our novel approach in [10, 23] is to introduce an extended state vector $\mathbf{x} = [x_1, x_2]^\top$, where $x_1 = x$ and $x_2 = -x$. By (1.1) and (1.4), one may verify that the dynamical system associated with the extended state vector $\mathbf{x} = [x_1, x_2]^\top$ has the governing field being a trigonometric polynomial with nonnegative frequencies only,

$$(3.3) \quad \frac{d}{dt} \begin{bmatrix} x_1 \\ x_2 \end{bmatrix} = \sum_{m=0}^M \begin{bmatrix} g_m \\ -g_m \end{bmatrix} e^{imx_1} + \sum_{m=1}^M \begin{bmatrix} g_{-m} \\ -g_{-m} \end{bmatrix} e^{imx_2}.$$

Set $y_\alpha = e^{i(\alpha_1 x_1 + \alpha_2 x_2)}$ for $\alpha = [\alpha_1, \alpha_2] \in \mathbb{Z}_+^2$. By (3.3), we have

$$(3.4) \quad \begin{aligned} \frac{dy_\alpha}{dt} &= iy_\alpha \left(\alpha_1 \frac{dx_1}{dt} + \alpha_2 \frac{dx_2}{dt} \right) \\ &= i(\alpha_1 - \alpha_2) \left(\sum_{m=0}^M g_m e^{imx_1} + \sum_{m=1}^M g_{-m} e^{imx_2} \right) y_\alpha \\ &= i(\alpha_1 - \alpha_2) \sum_{\beta \in \mathbb{Z}_+^2} h_{\beta-\alpha} y_\beta, \end{aligned}$$

where for $\gamma = [\gamma_1, \gamma_2]^\top \in \mathbb{Z}^2$ we define

$$(3.5) \quad h_\gamma = \begin{cases} g_{\gamma_1} & \text{if } 0 \leq \gamma_1 \leq M \text{ and } \gamma_2 = 0, \\ g_{-\gamma_2} & \text{if } \gamma_1 = 0 \text{ and } 1 \leq \gamma_2 \leq M, \\ 0 & \text{otherwise.} \end{cases}$$

For $\alpha = [\alpha_1, \alpha_2]^\top \in \mathbb{Z}^2$, denote its order by $|\alpha| = |\alpha_1| + |\alpha_2|$. Regrouping all equations in (3.4) with $|\alpha| = k$ yields

$$(3.6) \quad \frac{d\mathbf{y}_k}{dt} = \sum_{l=k}^{k+M} \mathbf{B}_{kl} \mathbf{y}_l$$

with initial $\mathbf{y}_k(0) = \mathbf{y}_k^0 = [e^{ikx_0}, e^{i(k-2)x_0}, \dots, e^{-i(k-2)x_0}, e^{-ikx_0}]^\top$, $k \geq 1$, where $\mathbf{y}_k = [y_\alpha]_{|\alpha|=k} = [e^{ikx_1}, e^{i((k-1)x_1+x_2)}, \dots, e^{i(x_1+(k-1)x_2)}, e^{ikx_2}]^\top$, and

$$(3.7) \quad \mathbf{B}_{kl} = [i(\alpha_1 - \alpha_2) h_{\beta-\alpha}]_{|\alpha|=k, |\beta|=l}, \quad 1 \leq k \leq l,$$

are block matrices depending on Fourier coefficients $g_{\pm(l-k)}$. The dynamical systems (3.6) can be rewritten as the following matrix formation:

$$(3.8) \quad \frac{d\mathbf{y}}{dt} := \frac{d}{dt} \begin{bmatrix} \mathbf{y}_1 \\ \mathbf{y}_2 \\ \vdots \\ \mathbf{y}_N \\ \vdots \end{bmatrix} = \begin{bmatrix} \mathbf{B}_{11} & \mathbf{B}_{12} & \cdots & \mathbf{B}_{1N} & \cdots \\ & \mathbf{B}_{22} & \cdots & \mathbf{B}_{2N} & \cdots \\ & & \ddots & \vdots & \ddots \\ & & & \mathbf{B}_{NN} & \ddots \\ & & & & \ddots \end{bmatrix} \begin{bmatrix} \mathbf{y}_1 \\ \mathbf{y}_2 \\ \vdots \\ \mathbf{y}_N \\ \vdots \end{bmatrix} =: \mathbf{By}$$

This revised linearization retains the fundamental benefits of the traditional Carleman techniques, such as a block-upper triangular state matrix, circumvents the structural

shortcomings associated with the direct Fourier-based linearization in (3.1). We call the infinite-dimensional dynamical system (3.8) as **Carleman-Fourier linearization** of the finite-dimensional nonlinear dynamical system (1.1) when the periodic vector field \mathbf{g} satisfies (1.4).

For the case that the governing function g has nonnegative frequencies only, i.e.,

$$(3.9) \quad g(x) = \sum_{m=0}^M g_m e^{imx},$$

we have

$$(3.10) \quad \frac{dz_k}{dt} = ik \sum_{l=k}^{M+k} g_{l-k} z_l$$

where $z_k = y_{[k,0]} = e^{ikx_1}$ is the first component of $\mathbf{y}_k, k \geq 1$ in (3.8). Then we can reformulate ODEs in (3.10) in the following matrix form,

$$(3.11) \quad \frac{d\mathbf{z}}{dt} = \mathbf{G}\mathbf{z}, \quad t \geq 0,$$

with initial condition $\mathbf{z}(0) = [e^{ikx_0}]_{k=1}^{\infty}$, where $\mathbf{z} = [z_1, z_2, \dots, z_N, \dots]^T$ and

$$(3.12) \quad \mathbf{G} = \begin{bmatrix} ig_0 & ig_1 & \dots & ig_{N-1} & \dots \\ 2ig_0 & \dots & 2ig_{N-2} & \dots \\ \ddots & \vdots & \ddots & \ddots \\ Nig_0 & \dots \\ \ddots & \ddots \end{bmatrix}.$$

As the state vector \mathbf{z} and the state matrix \mathbf{G} in (3.11) are parts of the state vector \mathbf{y} and the state matrix \mathbf{B} in the infinite-dimensional dynamical system (3.8) respectively, we call the infinite-dimensional linear system (3.11) as the **Carleman-Fourier linearization** of the dynamical system (1.1) when the governing function g has nonnegative frequencies only.

For the governing function in (1.6), one may verify that the corresponding Carleman-Fourier linearization is given by

$$(3.13) \quad \frac{d}{dt} \begin{bmatrix} z_1 \\ z_2 \\ z_3 \\ \vdots \\ z_{N-1} \\ z_N \\ \vdots \end{bmatrix} = ai \begin{bmatrix} 1 & -1 & 0 & \dots & 0 & 0 & \dots \\ 2 & -2 & \dots & 0 & 0 & 0 & \dots \\ 3 & \ddots & 0 & 0 & 0 & \dots \\ \ddots & \vdots & \vdots & \vdots & \vdots & \dots \\ N-1 & -N+1 & \dots & \dots & \dots & \dots \\ N & \dots & \dots & \dots & \dots & \dots \\ \ddots & \ddots & \ddots & \ddots & \ddots & \ddots \end{bmatrix} \begin{bmatrix} z_1 \\ z_2 \\ z_3 \\ \vdots \\ z_{N-1} \\ z_N \\ \vdots \end{bmatrix},$$

where the state matrix is an upper-triangular structure with bandwidth one.

4. FINITE-SECTION APPROXIMATION TO CARLEMAN-FOURIER LINEARIZATION

For the Carleman-Fourier linearization (3.8), we define its **finite-section approximation** of order $N \geq 1$ by

$$(4.1) \quad \frac{d}{dt} \begin{bmatrix} \mathbf{y}_{1,N} \\ \mathbf{y}_{2,N} \\ \vdots \\ \mathbf{y}_{N,N} \end{bmatrix} = \begin{bmatrix} \mathbf{B}_{11} & \mathbf{B}_{12} & \cdots & \mathbf{B}_{1N} \\ & \mathbf{B}_{22} & \cdots & \mathbf{B}_{2N} \\ & & \ddots & \vdots \\ & & & \mathbf{B}_{NN} \end{bmatrix} \begin{bmatrix} \mathbf{y}_{1,N} \\ \mathbf{y}_{2,N} \\ \vdots \\ \mathbf{y}_{N,N} \end{bmatrix} \quad \text{and } \mathbf{y}_{k,N}(0) = \begin{bmatrix} e^{ikx_0} \\ e^{i(k-2)x_0} \\ \vdots \\ e^{-ikx_0} \end{bmatrix}, \quad 1 \leq k \leq N.$$

By (3.5), (3.7) and (3.8), the finite-section approximation (4.1) of order $N = 1$ reduces to

$$\frac{d\mathbf{y}_{1,1}}{dt} = \begin{bmatrix} ig_0 & 0 \\ 0 & -ig_0 \end{bmatrix} \mathbf{y}_{1,1} \quad \text{and} \quad \mathbf{y}_{1,1}(0) = \begin{bmatrix} e^{ix_0} \\ e^{-ix_0} \end{bmatrix},$$

which has the solution

$$(4.2) \quad \mathbf{y}_{1,1}(t) = [e^{i(x_0+g_0t)}, e^{-i(x_0+g_0t)}]^T.$$

Similarly the finite-section approximation (4.1) of order $N = 2$ can be explicitly written as

$$\frac{d}{dt} \begin{bmatrix} \mathbf{y}_{1,2} \\ \mathbf{y}_{2,2} \end{bmatrix} = \begin{bmatrix} ig_0 & 0 & ig_1 & ig_{-1} & 0 \\ 0 & -ig_0 & 0 & -ig_1 & -ig_{-1} \\ 0 & 0 & 2ig_0 & 0 & 0 \\ 0 & 0 & 0 & 0 & 0 \\ 0 & 0 & 0 & 0 & -2ig_0 \end{bmatrix} \begin{bmatrix} \mathbf{y}_{1,2} \\ \mathbf{y}_{2,2} \end{bmatrix} \quad \text{and} \quad \begin{bmatrix} \mathbf{y}_{1,2}(0) \\ \mathbf{y}_{2,2}(0) \end{bmatrix} = \begin{bmatrix} e^{ix_0} \\ e^{-ix_0} \\ e^{2ix_0} \\ 1 \\ e^{-2ix_0} \end{bmatrix},$$

which has the solution given by

$$(4.3) \quad \begin{bmatrix} \mathbf{y}_{1,2}(t) \\ \mathbf{y}_{2,2}(t) \end{bmatrix} = \begin{bmatrix} (g_1 e^{i(2x_0+g_0t)} + g_{-1})(e^{ig_0t} - 1)/g_0 + e^{i(x_0+g_0t)} \\ (g_1 e^{-i(2x_0+g_0t)} + g_{-1})(e^{-ig_0t} - 1)/g_0 + e^{-i(x_0+g_0t)} \\ e^{2i(x_0+g_0t)} \\ 1 \\ e^{-2i(x_0+g_0t)} \end{bmatrix}.$$

The state matrix \mathbf{B} in the infinite-dimensional system (3.8) fails to be a bounded operator on the sequence space $\ell^2(\mathbb{Z}_{++}^2)$, rendering standard Hilbert space dynamical system theory inapplicable. However, as shown in the following theorem, the first block $\mathbf{y}_{1,N}$ in (4.1) still converges to the exponential $e^{i\mathbf{x}}$ of the extended state vector $\mathbf{x} = [x, -x]^T$ on a time range.

Theorem 4.1. [10] *Consider the dynamical system (1.1) governed by the periodic function g in (1.4), and the finite-section approximation (4.1) to its Carleman-Fourier linearization (3.8). Write $\mathbf{y}_{1,N} = [y_{1,N}^+, y_{1,N}^-]^T$ take $R > e$, and select the initial x_0 of the dynamical system (1.1) so that*

$$(4.4) \quad |\Im x_0| < \ln R - 1.$$

Then

$$(4.5) \quad |y_{1,N}^\pm(t) e^{\mp ix(t)} - 1| \leq C_0 N^{-3/2} e^{D_0(R)Nt} \left(\frac{\exp(|\Im x_0| + 1)}{R} \right)^{(e-1)N/(2e-1)}, \quad 0 \leq t \leq T_{CF}^*,$$

where $D_0(R) = 2 \max(|g_0|, (|g_1| + |g_{-1}|)R, \dots, (|g_M| + |g_{-M}|)R^M)$,

$$(4.6) \quad C_0 = \frac{1}{\sqrt{2\pi}(e-1)} \exp \left(\frac{3e-1}{2e-1} |\Im x_0| + \frac{3e-1}{2e-1} \ln R - \frac{e}{2e-1} \right),$$

and

$$(4.7) \quad T_{CF}^* = \frac{e-1}{(2e-1)D_0(R)} \ln \frac{R}{\exp(|\Im x_0| + 1)} > 0.$$

Take $T^{**} \leq T_{CF}^*$, and select a sufficiently large order N in the finite-section approximation (4.1) such that

$$(4.8) \quad C_0 N^{-3/2} e^{D_0(R)NT^{**}} \left(\frac{\exp(|\Im x_0| + 1)}{R} \right)^{(e-1)N/(2e-1)} \leq \frac{1}{2}.$$

Then $\xi_{1,N}^\pm(t) = -i \ln y_{1,N}^\pm(t)$, $0 \leq t \leq T^{**}$, with the initial $\xi_{1,N}^\pm(0) = \pm x_0$ is well defined by (4.5) and (4.8). This together with the observation

$$|z \bmod 2\pi| \leq 4\epsilon \quad \text{for all } z \in \mathbb{C} \text{ with } |e^{iz} - 1| \leq \epsilon \leq 1/2,$$

yields an exponential approximation to the state variable x for the dynamical system (1.1) by $\xi_{1,N}^\pm$ on the time range $[0, T^{**}]$,

$$(4.9) \quad \begin{aligned} & \max(|\xi_{1,N}^+(t) - x(t)|, |\xi_{1,N}^-(t) + x(t)|) \\ & \leq 4C_0 N^{-3/2} e^{D_0(R)Nt} \left(\frac{\exp(|\Im x_0| + 1)}{R} \right)^{(e-1)N/(2e-1)}, \quad 0 \leq t \leq T^{**}. \end{aligned}$$

For the Carleman-Fourier linearization (3.11) of dynamical systems with governing function having nonnegative frequencies, we define its finite-section approximation of order $N \geq 1$ by

$$(4.10) \quad \frac{d}{dt} \begin{bmatrix} z_{1,N} \\ z_{2,N} \\ \vdots \\ z_{N,N} \end{bmatrix} = \begin{bmatrix} ig_0 & ig_1 & \dots & ig_{N-1} \\ 2ig_0 & 2ig_1 & \dots & 2ig_{N-2} \\ \ddots & \ddots & \ddots & \vdots \\ & & & Nig_0 \end{bmatrix} \begin{bmatrix} z_{1,N} \\ z_{2,N} \\ \vdots \\ z_{N,N} \end{bmatrix} \quad \text{and} \quad \begin{bmatrix} z_{1,N}(0) \\ z_{2,N}(0) \\ \vdots \\ z_{N,N}(0) \end{bmatrix} = \begin{bmatrix} e^{ix_0} \\ e^{2ix_0} \\ \vdots \\ e^{Nix_0} \end{bmatrix}.$$

The finite-section approximation (4.10) of order $N \geq 1$ has solution $z_{1,1}(t) = e^{i(x_0 + g_0 t)}$ for $N = 1$, and $z_{1,2}(t) = g_1 e^{i(2x_0 + g_0 t)} (e^{ig_0 t} - 1)/g_0 + e^{i(x_0 + g_0 t)}$ for $N = 2$, cf. (4.2) and (4.3). As the state vector and matrix in the dynamical system (4.10) are subvector and submatrix of the finite-section approximation (4.1) respectively, we obtain from Theorem 4.1 that $z_{1,N}$ converges to the exponential e^{ix} of the state vector x of the original dynamical system in a time range.

Remark 4.2. We remark that for the case that the governing function g has nonnegative frequencies only, the first component $z_{1,N}$ in (4.10) may converge to the exponential e^{ix} in the entire time range $[0, \infty)$. In particular, it is shown in [10] that the above exponential convergence result for the finite-section approximation (4.10) has exponential convergence rate

$$(4.11) \quad \tilde{r}_{CF} = \frac{(D_0 + \mu_0) \|\exp(ix_0)\|_2}{\mu_0 R} < 1,$$

under the assumption that the zero-th Fourier coefficient g_0 and the initial x_0 satisfies

$$(4.12) \quad \mu_0 := \Im g_0 > 0 \quad \text{and} \quad \exp(-\Im x_0) < \frac{\mu_0 R}{D_0 + \mu_0},$$

where $R > \exp(|\Im x_0| + 1)$ and $D_0(R) = \max(|g_0|, |g_1|R, \dots, |g_M|R^M)$, c.f. (5.8). Under the assumption (4.12) on the governing function g and the initial state x_0 , imaginary part of the state vector $x(t)$ converges to positive infinity as $t \rightarrow \infty$ and the dynamical system associated with the new state vector e^{ix} (the exponential of the original state vector x) is stable.

For the case that the governing function g is given in (1.6), the corresponding finite-section approximation is given by

$$(4.13) \quad \frac{d}{dt} \begin{bmatrix} z_{1,N} \\ z_{2,N} \\ \vdots \\ z_{N-1,N} \\ z_{N,N} \end{bmatrix} = ai \begin{bmatrix} 1 & -1 & \dots & 0 & 0 \\ 2 & \dots & 0 & 0 & \\ \ddots & & \vdots & & \vdots \\ & & N-1 & -N+1 & \\ & & & & N \end{bmatrix} \begin{bmatrix} z_{1,N} \\ z_{2,N} \\ \vdots \\ z_{N-1,N} \\ z_{N,N} \end{bmatrix}$$

with initials $z_{k,N}(0) = \exp(ikx_0)$ for $1 \leq k \leq N$. By Theorem 4.1, we conclude that

$$(4.14) \quad |z_{1,N}(t)e^{-ix(t)} - 1| \leq C_0 N^{-3/2} e^{RNt} \left(\frac{\exp(|\Im x_0| + 1)}{R} \right)^{(e-1)N/(2e-1)}, \quad 0 \leq t \leq T_{CF}^*,$$

where R, C_0, T_{CF}^* are given by (4.4), (4.6) and (4.7) respectively with $D_0(R)$ replaced by $R \geq 1$. From the exponential convergence rate estimate in (4.14), we observe two key properties of the finite-section approximation (4.13) that its approximation error is **unaffected** by the real component of the initial condition x_0 , and that the approximation error **decreases** as the imaginary part of x_0 increases. This suggests that the finite-section approximation (4.13) possesses certain **global** convergence characteristics, a significant advantage over the **local** convergence characteristics of Carleman linearization shown in Theorem 2.1, and achieves rapid convergence under conditions where the dynamical system admits a satisfactory constant approximation.

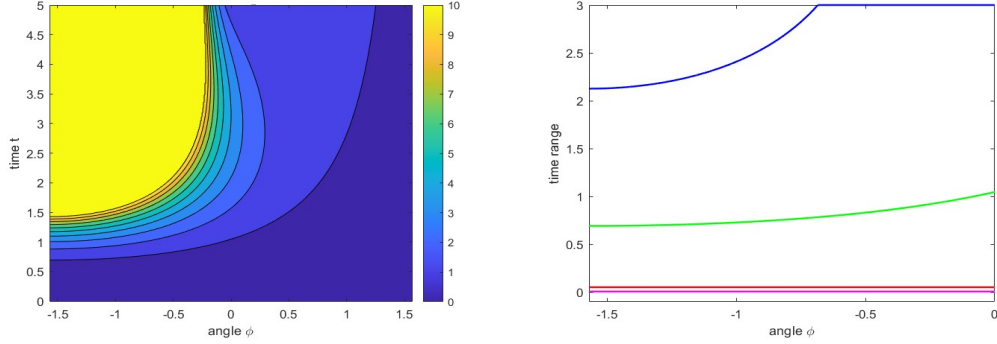


FIGURE 3. Plotted on the left is the function $\min\{h(\varphi, t), 10\}$, $-\pi/2 \leq \varphi \leq \pi/2$, $0 \leq t \leq 5$, where h is given in (5.4). Presented on the right is the actual time range $\min(T^*(\varphi), 3)$, $-\pi/2 \leq \varphi \leq 0$, in (5.6), where $\Im x_0 = 0$ (in green) and $\Im x_0 = 2$ (in blue), and the time range T_{CF}^* in Theorem 4.1 when $\Im x_0 = 0$ (in red) and when $\Im x_0 = 2$ (in magenta).

5. A CASE STUDY

In this section, we present a detailed case study on the finite-section approximation (4.13) when the original dynamical system has the governing function given in (1.6), and also compare the performance of finite-section approximations to its Carleman linearization and Carleman-Fourier linearization.

Let $z_{k,N}$, $1 \leq k \leq N$, be as in (4.13). By induction on $k = N, N-1, \dots, 1$, it can be verified that

$$(5.1) \quad z_{k,N}(t) = e^{ik(at+x_0)} \sum_{l=0}^{N-k} \frac{(k+l-1)!}{(k-1)!l!} \left(-e^{ix_0}(e^{iat}-1) \right)^l, \quad 1 \leq k \leq N.$$

Therefore the first component $z_{1,N}$ in the finite-section approximation (4.13) has the following explicit expression

$$(5.2) \quad z_{1,N}(t) = e^{i(at+x_0)} \sum_{l=0}^{N-1} \left(-e^{ix_0}(e^{iat}-1) \right)^l,$$

which is essentially the Taylor polynomial of order $N-1$ for the exponential function

$$e^{ix(t)} = e^{i(at+x_0)} \left(1 + e^{ix_0}(e^{iat}-1) \right)^{-1}$$

of the original state function $x(t)$ in (1.8). As a consequence of the explicit expression in (5.2), for any initial state x_0 and in the time range $[0, T^*]$, we have explicit approximation error

$$(5.3) \quad |z_{1,N}(t)e^{-ix(t)} - 1| = |e^{ix_0}(e^{iat}-1)|^N = e^{|\Im x_0|N} |e^{iat}-1|^N, \quad N \geq 1.$$

Write $a = e^{i\phi}$ as (1.7) and define

$$(5.4) \quad h(\phi, t) = |e^{iat} - 1|^2 = e^{-2t \sin \phi} - 2e^{-t \sin \phi} \cos(t \cos \phi) + 1, \quad t \geq 0,$$

see the left plot of Figure 3 for the function $\min(h(\phi, t), 10)$, $-\pi/2 \leq \phi \leq \pi/2, 0 \leq t \leq 5$. By (5.3), the first block, $z_{1,N}(t)$, $N \geq 1$, in the finite-section approximation (4.13) exhibits exponential convergence to $e^{ix(t)}$ in the time interval $[0, T^*)$ if and only if the requirement

$$(5.5) \quad h(\phi, t) < \exp(2\Im x_0) \quad \text{for all } 0 \leq t < T^*$$

is satisfied, c.f. (4.14).

In the case that $\phi \in [-\pi/2, 0)$, the function $h(\phi, t), t \geq 0$ is unbounded. Therefore, for any initial state x_0 , the actual time range

$$(5.6) \quad T^*(\phi) = \max\{T^* \mid (5.5) \text{ holds}\}$$

for the convergence of $z_{1,N}(t)$, $N \geq 1$, is finite. Illustrated in the right plot of Figure 3 are the maximal time range $\min(T^*(\phi), 5)$, $-\pi/2 \leq \phi \leq 0$, for $\Im x_0 = 0$ (in green) and $\Im x_0 = 2$ (in blue). We remark that the time range T_{CF}^* in (4.7), per Theorem 4.1, is given by

$$(5.7) \quad T_{CF}^* = \sup_{\ln R > |\Im x_0| + 1} \frac{e - 1}{(2e - 1)R} (\ln R - |\Im x_0| - 1) = \frac{e - 1}{(2e - 1)} e^{-|\Im x_0| - 2}$$

see the right plot of Figure 3, where $T_{CF}^* \approx 0.0524$ for $\Im x_0 = 0$ (in red) and $T_{CF}^* \approx 0.0071$ for $\Im x_0 = 2$ (in magenta). We observe that the time range T_{CF}^* in (4.7) is independent on the selection of $a = \exp(i\phi)$, and it is much smaller than the actual time range $T^*(\phi)$, $-\pi/2 \leq \phi < 0$, for the exponential convergence of the finite-section approximation to the Carleman-Fourier linearization. Accordingly, the theoretical bound on the time range T_{CF}^* in (4.7) should be considered as a conservative guarantee of exponential convergence for the finite-section approximation, rather than as a precise or sharp description of the actual time range.

For the scenarios when $\phi = 0$, implying $a = 1$ or equivalently $\Im a = 0$, it can be verified that the maximum time range for the convergence of $z_{1,N}(t)$ can be evaluated explicitly,

$$T^*(\phi) = \begin{cases} 2 \arcsin \frac{\exp(\Im x_0)}{2} & \text{if } \Im x_0 \leq \ln 2 \\ +\infty & \text{otherwise.} \end{cases}$$

Illustrated in the right plot of Figure 3 is $T^*(0) \approx \pi/3 \approx 1.0472$ for $\Im x_0 = 0$ (in red) and $T^*(0) = +\infty$ for $\Im x_0 = 2$ (in blue).

For the case when $\phi \in (0, \pi/2]$, we have $0 \leq h(\phi, t) \leq 4$. Using (5.2), we can conclude that $z_{1,N}(t)$, $N \geq 1$ in the finite-section approximation (4.13) provides a satisfactory approximation to $e^{ix(t)}$ over the **entire time range** $[0, \infty)$, provided that

$$(5.8) \quad \Im x_0 > \frac{1}{2} \ln h(\phi, t) \quad \text{for all } t \geq 0,$$

which is the region above the green line on the right plot of Figure 3, c.f. Remark 4.2.

Figures 4 depicts the approximation performance of the finite-section approach (4.13), where $a = e^{i\phi}$ and

$$\begin{aligned} E_{CF}(x_0, T^*, N) &= \max_{0 \leq t \leq T^*} \log_{10} |z_{1,N}(t)e^{-ix(t)} - 1| \\ (5.9) \quad &= N \left(-\Im x_0 \log_{10} e + \frac{1}{2} \log_{10} \left(\max_{0 \leq t \leq T^*} h(\phi, t) \right) \right). \end{aligned}$$

This demonstrates that the first component $z_{1,N}(t)$ in the finite-section approximation (4.13) provides a better approximation to the original state $x(t)$ of the dynamical system (1.6) in a longer time range when $\phi \in [-\pi/2, 0)$ and in the whole time range $[0, \infty)$ when $\phi \in (0, \pi/2]$, provided that the imaginary $\Im x_0$ of initial state x_0 takes larger value. It is also observed that the proposed Carleman-Fourier linearization has better performance for the complex dynamical system (1.6) with the parameter a having positive imaginary part than for the one with the parameter a having negative imaginary part. We believe that the possible reason is that the finite-section approximation (4.13) associated with the Carleman-Fourier linearization of the corresponding dynamical system is stable when $\Im a < 0$, while it is unstable when $\Im a > 0$.

5.1. Comparison between Carleman and Carleman-Fourier linearization. Our numerical simulations show that the finite-section approximation of the Carleman-Fourier linearization exhibits exponential convergence on the entire range if $\Im a \geq 0$ and $\Im x_0 > \ln 2$, while the finite-section approximation of the Carleman linearization has exponential convergence on the entire range when $\Im a < 0$. The possible reason is that the dynamical system (1.6) associated with the finite-section approximation of the Carleman-Fourier linearization is stable when $\Im a > 0$, while the dynamical system (1.6) associated with the finite-section approximation of the Carleman linearization is stable when $\Im a < 0$.

Comparing the performance between the Carleman-Fourier linearization and the Carleman linearization shown in Figures 1 and 4, we see that the proposed Carleman-Fourier linearization has much better performance than the Carleman linearization when $\Im x_0$ is large and the governing field is well approximated by trigonometric polynomials, while the Carleman linearization, as expected, is a superior linearization technique of a nonlinear dynamical system when the initial is not far from the origin.

APPENDIX A. A DYNAMICAL SYSTEM WITH PERIODIC GOVERNING FUNCTION

In this appendix, we consider the trajectory behaviour of the dynamical system (1.6), which could blow up at a finite time, exhibit a limit cycle, and converge or diverge, see Figure 5.

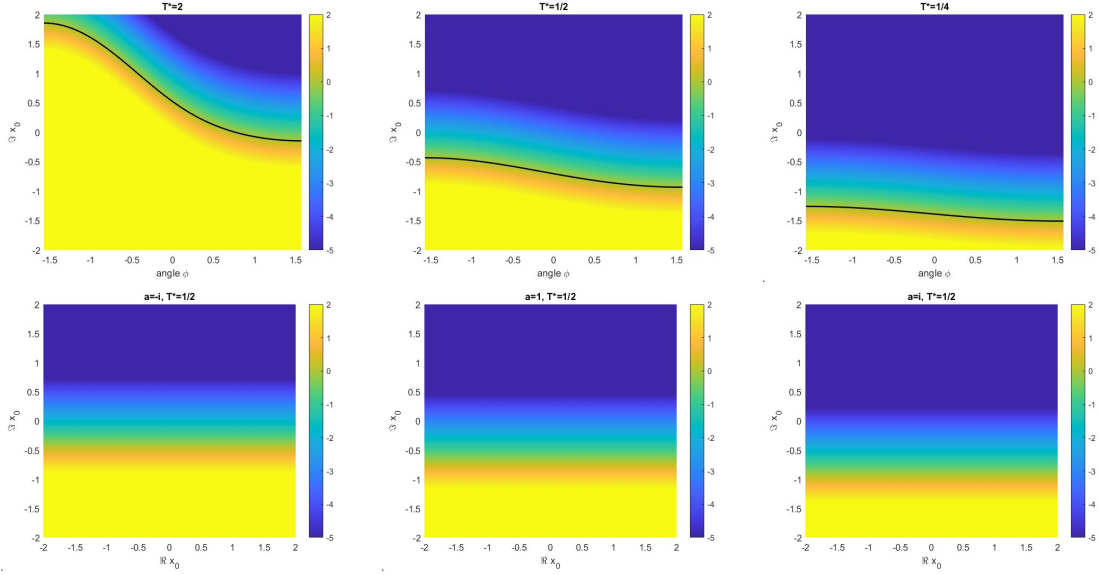


FIGURE 4. Plotted on the top are the finite-section approximation errors $\max(\min(E_{CF}(x_0, T^*, N), 2), -5)$ with $\pi/2 \leq \phi \leq \pi/2$ as the x -axis and $-2 \leq \Im x_0 \leq 2$ as the y -axis, and level curve $E_{CF}(x_0, T^*, N) = 0$ (in black) for $N = 10$ and $T^* = 2$ (left), $1/2$ (middle) and $1/4$ (right) respectively. Shown on the bottom are $\max(\min(E_{CF}(x_0, T^*, N), 2), -5)$ with $-\pi/2 \leq \Re x_0 \leq 2$ as the x -axis and $-2 \leq \Im x_0 \leq 2$ as the y -axis, for $N = 10, T^* = 1/2$ and $\phi = -\pi/2$ (left), 0 (middle) and $\pi/2$ (right) respectively.

By (1.8), the solution $x(t)$ of the complex dynamical system (1.6) may blow up at a finite time $t = t_0 > 0$ if the initial x_0 satisfies

$$(A.1) \quad 1 + (e^{ait_0} - 1)e^{ix_0} = 0 \quad \text{and} \quad 1 + (e^{ait} - 1)e^{ix_0} \neq 0 \quad \text{for all } 0 \leq t < t_0,$$

see the black trajectories shown in Figure 5 where simulation parameters $x_0 = i \ln(1 - e^{a i \pi/2})$ for $a = 1, i, -i$ respectively. One may verify that the requirement (A.1) for the initial state vector x_0 is met for some $t_0 > 0$ when $\Re(e^{ix_0}) = \frac{1}{2}$ and $a = 1$, or when $\Re x_0 \in 2\pi\mathbb{Z} + \pi$ and $a = -i$, or when $\Re x_0 \in 2\pi\mathbb{Z}$ and $\Im x_0 < 0$ and $a = i$.

Now we continue examining the behavior of the dynamical system (1.6) when the initial vector x_0 does not satisfy condition (A.1) for all $t_0 > 0$, i.e., $1 + (e^{ait} - 1)e^{ix_0} \neq 0$ for all $t \geq 0$. For the case that $\Im a = 0$, i.e., $a = 1$, we observe that $e^{-ix_0}(1 + (e^{it} - 1)e^{ix_0}), t \geq 0$, is a circle with center $e^{-ix_0} - 1$ and radius 1. Therefore $\ln(1 - (e^{it} - 1)e^{ix_0})$ is a periodic function with a period of 2π when $|e^{-ix_0} - 1| > 1$, and $\ln(1 - b(e^{it} - 1)) - it$ is a periodic function with the same period of 2π when $|e^{-ix_0} - 1| < 1$. This implies that when $a = 1$, the dynamical system (1.6) diverges when $|e^{-ix_0} - 1| < 1$ and exhibits a limit cycle when $|e^{-ix_0} - 1| > 1$. These behaviors

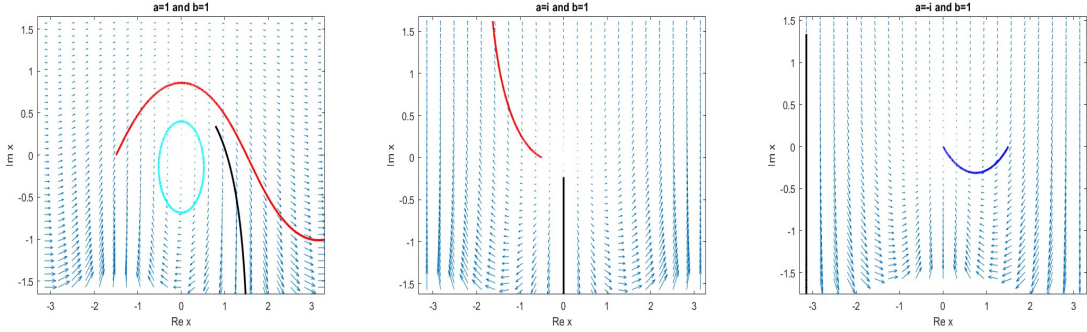


FIGURE 5. Plotted are the vector fields $a(1 - e^{ix})$ of the complex dynamical system (1.6) with $a = 1$ (left), $a = i$ (middle) and $a = -i$ (right), where $-\pi \leq \Re x \leq \pi$ and $-\pi/2 \leq \Im x \leq \pi/2$. Trajectories on the left figure has parameter $a = 1$ (left) and initial $x_0 = i \ln(1 - e^{ai\pi/2}) \approx 0.7854a + 0.3466i$ (in black), $-1/2a$ (in cyan) and $-3/2a$ (in red). Presented in the middle is trajectories with $a = i$ and $x_0 = i \ln(1 - e^{ai\pi/2}) \approx -0.2330i$ (in black) and $-1/2$ (in red), while on the right are trajectories with $a = -i$ and $x_0 = i \ln(1 - e^{ai\pi/2}) \approx -3.1416 + 1.3378i$ (in black) and $3/2$ (in blue). Trajectories shown in the figures may blow up in a finite time (in black), have limit cycle (in cyan), converge (in blue) and diverge (in red).

are illustrated by the cyan color limit cycle trajectory in Figure 5 with a period of 2π and the red color trajectory in Figure 5, where $x(t) - t$ forms a periodic function with a period of 2π .

For the case that $\Im a \neq 0$, we observe that (i) $\lim_{t \rightarrow \infty} 1 + e^{ix_0}(e^{ait} - 1) = 1 - e^{ix_0}$ when $\Im a > 0$; and (ii) $\lim_{t \rightarrow \infty} e^{-iat} (1 + e^{ix_0}(e^{ait} - 1)) = e^{ix_0}$ when $\Im a < 0$. Therefore, the dynamical system (1.6) converges when $\Im a < 0$, diverges when $\Im a > 0$ and $x_0 \notin 2\pi\mathbb{Z}$, and the solution of the dynamical system (1.6) remains at the equilibrium $x_0 \in 2\pi\mathbb{Z}$. This behavior is illustrated by the green color trajectory in the right plot of Figure 5, and the red color trajectory in the middle plot of Figure 5.

APPENDIX B. PROOF OF THEOREM 2.1

In this appendix, we adopt the procedure outlined in [2] to establish Theorem 2.1, under modified assumptions on the Taylor coefficients of the governing function. First, we need a local bound estimate for the state vector x of the dynamical system (2.8).

Lemma B.1. *For any given $M_0 > |x_0|$, we have*

$$(B.1) \quad |x(t)| \leq M_0 \quad \text{for all } 0 \leq t \leq \frac{M_0 R_0}{C_0(e^{R_0 M_0} - 1)} \ln \frac{M_0}{|x_0|},$$

where C_0 and R_0 are constants in (2.9).

Proof. By the continuity of the state vector x , either $|x(t)| \leq M_0$ for all $t \geq 0$ or there exists some $T > 0$ such that $|x(t)| \leq M_0$ for all $0 \leq t \leq T$ and $|x(T)| = M_0$. Clearly it suffices to prove

$$(B.2) \quad T \geq \frac{M_0 R_0}{C_0(e^{R_0 M_0} - 1)} \ln \frac{M_0}{|x_0|}$$

for the second case. Observe that

$$\begin{aligned} |x(t)| &\leq |x_0| + \int_0^t |f(s)| ds \leq |x_0| + \sum_{n=1}^{\infty} |c_n| \int_0^t |x(s)|^n ds \\ &\leq |x_0| + \sum_{n=1}^{\infty} \frac{C_0 R_0^{n-1}}{n!} M_0^{n-1} \int_0^t |x(s)| ds \\ &= |x_0| + \frac{C_0(e^{M_0 R_0} - 1)}{M_0 R_0} \int_0^t |x(s)| ds \quad \text{for all } 0 \leq t \leq T, \end{aligned}$$

which implies that

$$\exp\left(-\frac{C_0(e^{M_0 R_0} - 1)}{M_0 R_0} t\right) \left(\int_0^t |x(s)| ds + \frac{M_0 R_0 |x_0|}{C_0(e^{M_0 R_0} - 1)} \right)$$

is a decreasing function on $[0, T]$. Hence

$$|x(t)| \leq |x_0| \exp\left(\frac{C_0(e^{M_0 R_0} - 1)}{M_0 R_0} t\right) \quad \text{for all } 0 \leq t \leq T.$$

This together with the assumption $|x(T)| = M_0$ of the second case proves (B.2) and completes the proof. \square

Now we start the proof of Theorem 2.1.

Proof of Theorem 2.1. Let $x_{k,N}$, $1 \leq k \leq N$, be as in (2.14) and set $y_k(t) = (x(t))^k - x_{k,N}(t)$, $1 \leq k \leq N$. Then, y_k , $1 \leq k \leq N$, satisfy the following ODEs,

$$\frac{dy_k}{dt} = k c_1 y_k + \sum_{n=k+1}^N k c_{n-k+1} y_n + \sum_{n=N+1}^{\infty} k c_{n-k+1} x^n$$

with initials $y_k(0) = 0$. Multiplying $\exp(-c_1 k t)$ at both sides of the above ODEs and then integrating, we obtain

$$y_k(t) = k \int_0^t e^{c_1 k(t-s)} \left[\sum_{n=k+1}^N c_{n-k+1} y_n(s) + \sum_{n=N+1}^{\infty} c_{n-k+1} (x(s))^n \right] ds.$$

Take $M_0 > |x_0|$ and set $T = \frac{M_0 R_0}{C_0(e^{M_0 R_0} - 1)} \ln \frac{M_0}{|x_0|}$. Therefore for all $0 \leq t \leq T$ and $1 \leq k \leq N$, we obtain from (2.9) and Lemma B.1 that

$$\begin{aligned} |y_k(t)| &\leq C_0 k \int_0^t e^{C_0 k(t-s)} \left[\sum_{n=k+1}^N \frac{R_0^{n-k}}{(n-k+1)!} |y_n(s)| + \sum_{n=N+1}^{\infty} \frac{M_0^n R_0^{n-k}}{(n-k+1)!} \right] ds \\ (B.3) \quad &\leq C_0 k \int_0^t e^{C_0 k(t-s)} \left[\sum_{n=k+1}^N \frac{R_0^{n-k}}{(n-k+1)!} |y_n(s)| + \frac{(e^{M_0 R_0} - 1) M_0^N R_0^{N-k}}{(N+1-k)!} \right] ds, \end{aligned}$$

where the last estimate holds as

$$\begin{aligned} \sum_{n=N+1}^{\infty} \frac{M_0^n R_0^{n-k}}{(n-k+1)!} &= \sum_{m=0}^{\infty} \frac{M_0^{m+N+1} R_0^{m-k+N+1}}{(N+1+m-k+1)!} \\ &\leq \frac{M_0^N R_0^{N-k}}{(N+1-k)!} \sum_{m=0}^{\infty} \frac{M_0^{m+1} R_0^{m+1}}{(m+1)!} = \frac{(e^{M_0 R_0} - 1) M_0^N R_0^{N-k}}{(N+1-k)!}. \end{aligned}$$

Let $\tilde{R}_0 = \max(1, R_0 |x_0| e^2)$ as in (2.11) and set

$$u_k(t) = (e^{M_0 R_0} - 1)^{-1} M_0^{-N} (R_0 / \tilde{R}_0)^{k-N} |y_k(t)|, \quad 1 \leq k \leq N.$$

Then, for $1 \leq k \leq N$, we obtain from (B.3) that

$$\begin{aligned} u_k(t) &\leq C_0 k K \int_0^t e^{C_0 k(t-s)} \left[\sum_{n=k+1}^N u_n(s) + 1 \right] ds \\ (B.4) \quad &\leq C_0 k K \int_0^t e^{C_0 k K(t-s)} \left[\sum_{n=k+1}^N u_n(s) + 1 \right] ds, \end{aligned}$$

where

$$(B.5) \quad 1 \leq K := \sup_{m \geq 0} \frac{\tilde{R}_0^m}{(m+1)!} \leq \sum_{m=0}^{\infty} \frac{\tilde{R}_0^m}{(m+1)!} = \frac{e^{\tilde{R}_0} - 1}{\tilde{R}_0} \leq e^{\tilde{R}_0} / \tilde{R}_0.$$

Taking $k = N$ in (B.4) gives

$$u_N(t) + 1 \leq e^{C_0 K N t}, \quad 0 \leq t \leq T.$$

By induction on $k = N, N-1, \dots, 2$, we can show that

$$(B.6) \quad \sum_{n=k}^N u_n(t) + 1 \leq \frac{N^{N-k}}{(N-k)!} e^{C_0 K N t}, \quad 0 \leq t \leq T.$$

Substituting the above estimate with $k = 2$ into the right hand side of the estimate (B.4) with $k = 1$ gives

$$\begin{aligned} u_1(t) &\leq C_0 K \frac{N^{N-2}}{(N-2)!} \int_0^t e^{C_0 K(t-s)} e^{C_0 K N s} ds \\ (B.7) \quad &\leq \frac{N^{N-2}}{(N-1)!} e^{C_0 K N t} \leq (2\pi)^{-1/2} N^{-3/2} e^{N+C_0 K N t}, \quad 0 \leq t \leq T, \end{aligned}$$

where we use the Stirling inequality $N! > \sqrt{2\pi} N^{N+1/2} e^{-N}$. Therefore

$$(B.8) \quad |y_1(t)| \leq \frac{(e^{M_0 R_0} - 1) \tilde{R}_0}{\sqrt{2\pi} R_0} N^{-3/2} \left(\frac{M_0 R_0 e^{C_0 e^{\tilde{R}_0} t / \tilde{R}_0}}{\tilde{R}_0} \right)^N.$$

Let T^* be as in (2.12), fix $0 < t < T^*$, and set $M_0 = |x_0| \exp(C_0 e^{\tilde{R}_0} t)$. Then $M_0 R_0 \leq R_0 |x_0| e^2 \leq \tilde{R}_0$ and

$$\frac{M_0 R_0}{C_0 (e^{M_0 R_0} - 1)} \ln \frac{M_0}{|x_0|} \geq \frac{M_0 R_0 e^{\tilde{R}_0}}{e^{M_0 R_0} - 1} t \geq t.$$

Therefore

$$|x(s)| \leq M_0 \quad \text{for all } 0 \leq s \leq t$$

by Lemma B.1. Then applying (B.8) with the above selection of M_0 yields

$$|y_1(s)| \leq \frac{\tilde{R}_0 e^{\tilde{R}_0}}{\sqrt{2\pi} R_0} N^{-3/2} \left(\frac{R_0 |x_0| e^{C_0 e^{\tilde{R}_0} (t+s/\tilde{R}_0)}}{\tilde{R}_0} \right)^N \quad \text{for all } 0 \leq s \leq t.$$

The desired estimate (2.10) follows from the above inequality by taking $s = t$. \square

REFERENCES

- [1] M. Abudia, J. A. Rosenfeld and R. Kamalapurkar, Carleman lifting for nonlinear system identification with guaranteed error bounds, *2023 American Control Conference (ACC)*, IEEE, 2023, pp. 929–934.
- [2] A. Amini, C. Zheng, Q. Sun and N. Mottee, Carleman linearization of nonlinear systems and its finite-section approximations, *Discrete Con. Dyn. Ser B.*, vol. 30(2), 2025, pp. 577–603.
- [3] A. Amini, Q. Sun and N. Mottee, Error bounds for Carleman linearization of general nonlinear systems, *2021 Proc. the Conference on Control and its Applications*, SIAM, 2021, pp. 1–8.
- [4] A. Amini, Q. Sun and N. Mottee, Approximate optimal control design for a class of nonlinear systems by lifting Hamilton-Jacobi-Bellman equation, *2020 American Control Conference (ACC)*, IEEE, 2020, pp. 2717–2722.
- [5] A. Amini, Q. Sun and N. Mottee, Quadratization of Hamilton-Jacobi-Bellman equation for near-optimal control of nonlinear systems, *59th IEEE Conference on Decision and Control (CDC)*, IEEE, 2020, pp. 731–736.
- [6] T. Akiba, Y. Morii and K. Maruta, Carleman linearization approach for chemical kinetics integration toward quantum computation, *Sci. Rep.*, vol. 13(1), 2023, article no. 3935, 10 pp.
- [7] M.-A. Belabbas and X. Chen, A sufficient condition for the super-linearization of polynomial systems, *Control Syst. Lett.*, vol. 179, 2023, article no. 105588, 6 pp.

- [8] R. Brockett, The early days of geometric nonlinear control, *Automatica*, vol. 50(9), 2014, pp. 2203–2224.
- [9] S. L. Brunton, J. L. Proctor and J. N. Kutz, Discovering governing equations from data by sparse identification of nonlinear dynamical systems, *Proc. Natl. Acad. Sci. U.S.A.*, vol. 113(15), 2016, pp. 3932–3937.
- [10] P. Chen, N. Motee and Q. Sun, Carleman-Fourier linearization of complex dynamical systems: convergence and explicit error bounds, arXiv:2411.11598, 2024.
- [11] M. Forets and A. Pouly, Explicit error bounds for Carleman linearization, 2017, *arXiv:1711.02552*, 2017.
- [12] M. Forets and C. Schilling, Reachability of weakly nonlinear systems using Carleman linearization, *International Conference on Reachability Problems*, Springer, 2021, pp. 85–99.
- [13] J. Gonzalez-Conde, D. Lewis, S. S. Bharadwaj and M. Sanz, Quantum Carleman linearization efficiency in nonlinear fluid dynamics, *Phys. Rev. Research*, vol. 7, 2025, article no. 023254, 16 pp.
- [14] A. Harshana and M.-A. Belabbas, On the invariance of super-linearization under polynomial automorphisms, arXiv:2503.13849, 2025.
- [15] N. Hashemian and A. Armaou, Fast moving horizon estimation of nonlinear processes via Carleman linearization, *2015 American Control Conference (ACC)*, IEEE, 2015, pp. 3379–3385.
- [16] M. Korda and I. Mezić, Linear predictors for nonlinear dynamical systems: Koopman operator meets model predictive control, *Automatica*, vol. 93, 2018, pp. 149–160.
- [17] M. Korda and I. Mezić, On convergence of extended dynamic mode decomposition to the Koopman operator, *J. Nonlinear Sci.*, vol. 28, 2018, pp. 687–710.
- [18] K. Kowalski and W.H. Steeb, *Nonlinear Dynamical Systems and Carleman Linearization*, World Scientific, 1991.
- [19] A. J. Krener, Linearization and bilinearization of control systems, *Proceedings of the 1974 Allerton Conference on Circuit and Systems Theory, Urbana III*, 1974, 11 pp.
- [20] J.P. Liu, H. O. Kolden, H. K. Krovi, N. F. Loureiro, K. Trivisa and A. W. Childs, Efficient quantum algorithm for dissipative nonlinear differential equations, *Proc. Natl. Acad. Sci. U.S.A.*, vol. 118(35), 2021, article no. e2026805118, 6 pp.
- [21] K. Loparo and G. Blankenship, Estimating the domain of attraction of nonlinear feedback systems, *IEEE Trans. Automat. Contr.*, vol. 23(4), 1978, pp. 602–608.
- [22] J. Minisini, A. Rauh and E. P. Hofer, Carleman linearization for approximate solutions of nonlinear control problems: Part 1–theory, *Proc. of the 14th International Workshop on Dynamics and Control*, 2007, pp. 215–222.
- [23] N. Motee and Q. Sun, Carleman-Fourier linearization of nonlinear real dynamical systems, *Discrete and Continuous Dynamical Systems - B*, to appear, Doi 10.3934/dcdsb.2025168
- [24] S. Pruekprasert, J. Dubut, T. Takisaka, C. Eberhart and A. Cetinkaya, Moment propagation through Carleman linearization with application to probabilistic safety analysis, *Automatica*, vol. 160, 2024, paper no. 111441, 13 pp.
- [25] A. Rauh, J. Minisini and H. Aschemann, Carleman linearization for control and for state and disturbance estimation of nonlinear dynamical processes, *IFAC Proc. Vol.*, vol. 42(13), 2009, pp. 455–460.
- [26] D. Rotondo, G. Luta and J. H. U. Aarvag, Towards a Taylor-Carleman bilinearization approach for the design of nonlinear state-feedback controllers, *Eur. J. Control*, vol. 68, 2022, article no. 100670, 8 pp.
- [27] W. H. Steeb and F. Wilhelm, Non-linear autonomous systems of differential equations and Carleman linearization procedure, *J. Math. Anal. Appl.*, vol. 77(2), 1980, pp. 601–611.

- [28] A. Surana, A. Gnanasekaran and T. Sahai, An efficient quantum algorithm for simulating polynomial dynamical systems, *Quantum Inf. Process.*, vol. 23(3), 2024, article no. 105, 22 pp.
- [29] T. A. Vaszary, Carleman linearization of partial differential equations, *arXiv:2412.00014*, 2024.
- [30] Z. Wang, R. M. Jungers and C. J. Ong, Computation of invariant sets via immersion for discrete-time nonlinear systems, *Automatica*, vol. 147, 2023, article no. 110686, 9 pp.
- [31] H. C. Wu, J. Wang and X. Li, Quantum algorithms for nonlinear dynamics: revisiting Carleman linearization with no dissipative conditions, *SIAM J. Sci. Comput.*, vol. 47, 2025, pp. A943–A970.

DEPARTMENT OF MATHEMATICS, UNIVERSITY OF CENTRAL FLORIDA, ORLANDO, FLORIDA 32816

Email address: panpan.chen@ucf.edu

MECHANICAL ENGINEERING AND MECHANICS, LEHIGH UNIVERSITY, BETHLEHEM, PA 18015
Email address: nam211@lehigh.edu

DEPARTMENT OF MATHEMATICS, UNIVERSITY OF CENTRAL FLORIDA, ORLANDO, FLORIDA 32816

Email address: qiyu.sun@ucf.edu